ARTICLES
PUBLISHED ONLINE: 22 JANUARY 2012 | DOI: 10.1038/NMAT3222
nature materials

Synthetic mast-cell granules as adjuvants to promote and polarize immunity in lymph nodes

Ashley L. St. John[1]*†, Cheryl Y. Chan[2], Herman F. Staats[1,2,3], Kam W. Leong[4] and Soman N. Abraham[1,2,5,6]

Granules of mast cells (MCs) enhance adaptive immunity when, on activation, they are released as stable particles. Here we show that submicrometre particles modelled after MC granules augment immunity when used as adjuvants in vaccines. The synthetic particles, which consist of a carbohydrate backbone with encapsulated inflammatory mediators such as tumour necrosis factor, replicate attributes of MCs *in vivo* including the targeting of draining lymph nodes and the timed release of the encapsulated mediators. When used as an adjuvant during vaccination of mice with haemagglutinin from the influenza virus, the particles enhanced adaptive immune responses and increased survival of mice on lethal challenge. Furthermore, differential loading of the particles with the cytokine IL-12 directed the character of the response towards Th1 lymphocytes. The synthetic MC adjuvants replicate and enhance the functions of MCs during vaccination, and can be extended to polarize the resulting immunity.

Adjuvants are added to vaccine formulations to enhance the host memory response to an antigen when administered in conjunction with that antigen. There is currently an urgent need to develop adjuvants that are effective and versatile in modulating immune responses, and that can be tailored to elicit a specific response to counter a unique challenge, such as an infectious disease or cancer. Under these circumstances, the most effective response may be not only maximized but also polarized, defined by a profile of certain cytokines, antibodies and other humoural factors. These considerations are hardly addressed by currently approved vaccination strategies. Although the adaptive immune response that protects an individual from a challenge after vaccination is initiated and refined in draining lymph nodes (LNs), all currently approved adjuvants are thought to enhance immunity through their effects in a distal site where antigen is injected[1]. For example, the described mechanisms of the actions of MF59, CpG or alum are largely confined to the site of vaccine administration, either by influencing the persistence of antigen or by modulating the function of dendritic cells (DCs; ref. 1). The activation of DCs is one of the most important initiating events in the adaptive immune response. However, the trafficking of these cells to the draining LN, their subsequent interactions with LN-resident lymphocytes and the activation and interactions of lymphocytes themselves are also essential to the amplification of adaptive immunity and the formation of protective immunological memory[2]. This makes LN targeting of antigen—or of antigen-activated immune cells—and induction of LN remodelling highly desirable traits of a candidate adjuvant.

Optimal immunity relies on rapid communication between the periphery and the draining LN during natural infection, in part through the actions of MCs, which can influence DC migration and the inflammatory milieu of the draining LN, resulting in heightened antibody responses[3,4]. MCs release stable particles in response to various stimuli, including pathogens[5], and we have shown that these particles retain inflammatory mediators and travel with them to the draining LNs (ref. 6). Tumour necrosis factor (TNF), for example, remains associated with the particles after exocytosis and drastically reorganizes draining LNs, being responsible for the initial swelling during bacterial infection, where LNs double in size[6]. It is likely that the targeting of products by exocytosed granules to LNs also contributes to other processes that are influenced by MCs, including the development of high-affinity antibodies. In support of this hypothesis, compounds that have the capacity to activate MCs can act as vaccine adjuvants[7]. Thus far, efforts to apply adjuvants to vaccine formulations have focused on enhancing the magnitude of immune responses. However, the character of the resulting immune response can also influence the success of a vaccine strategy in preventing illness, which is highly pathogen dependent. MC-promoted responses have been predominantly characterized as Th2 responses, defined by efficient antibody production and high levels of cytokines including IL-4. In contrast, Th1-type responses have been shown to be most effective in protection against intracellular pathogens owing to the efficient induction of cytotoxic T cells. These responses are characterized by IL-12-promoted production of interferon-γ (IFN-γ), particularly by T cells. Although T-cell polarization is defined by a vast literature, a central reoccurring theme is that the cytokine profile during activation can determine the resulting type of functional adaptive immune response.

Cytokines themselves can be used as effective adjuvants, although significant quantities of mediators are required to achieve

[1]Department of Immunology, Duke University Medical Center, Durham, North Carolina 27710, USA, [2]Department of Pathology, Duke University Medical Center, Durham, North Carolina 27710, USA, [3]Department of Medicine, Duke University Medical Center, Durham, North Carolina 27710, USA, [4]Department of Biomedical Engineering, Duke University Medical Center, Durham, North Carolina 27710, USA, [5]Department of Molecular Genetics and Microbiology, Duke University Medical Center, Durham, North Carolina 27710, USA, [6]Program in Emerging Infectious Diseases, Duke-National University of Singapore, Singapore 169857, Singapore. †Present addresses: Program in Emerging Infectious Diseases, Duke-National University of Singapore, Graduate Medical School, Level 9, Khoo Teck Puat Building, 8 College Road, Singapore 169857, Singapore; Department of Pathology, Duke University Medical Center, Durham, North Carolina 27710, USA. *e-mail: ashley.st.john@duke.edu.

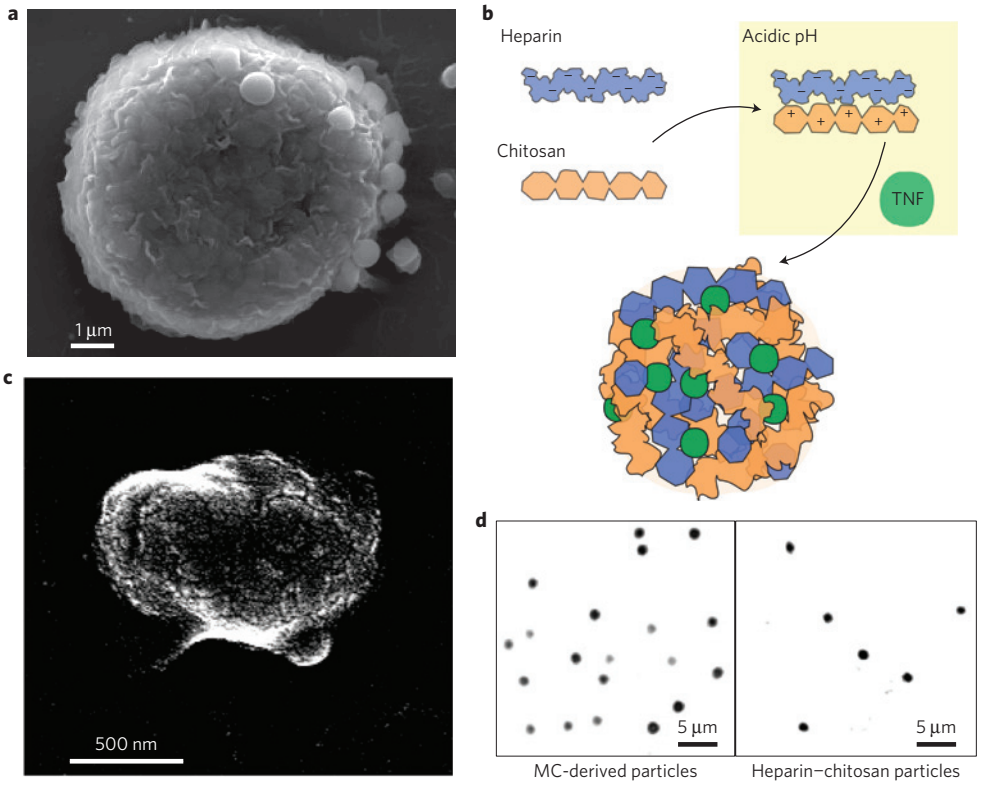

Figure 1 | Synthetic particles are modelled after MC-derived particles. a, Scanning electron micrograph of an activated rat peritoneal MC, partially degranulated. **b**, Diagram demonstrating the modelling of synthetic particles after MC granules, where chitosan, made positively charged under acidic conditions, is substituted for MC proteases, enabling inflammatory mediators to be entrapped within a similar matrix structure containing heparin. **c**, Scanning electron micrograph of an individual synthetic particle consisting of heparin and chitosan. **d**, Comparison of MC-derived particles and synthetic particles by light microscopy. Images were acquired with ×100 magnification.

observable effects[8]. They are costly to produce and frequently have adverse side-effects when injected *in vivo* in soluble form at effective concentrations[9,10]. Hence, exocytosed MC granules can be thought of as acting as physiological drug-delivery devices, ensuring that minute quantities of pro-inflammatory mediators are efficiently delivered directly to the draining LNs in a form protected from degradation and dilution to promote the adaptive immune process. We therefore proposed to harness and extend the MC strategy to maximize or polarize immunity through targeted delivery of similar mediator-containing particles.

Particle design as modelled after MC granules

Natural MC-derived particles consist primarily of carbohydrates, specifically heparin, and proteases, and are formed by the process of polyelectrolyte complexation occurring at the cellular level, where submicrometre-sized structures are held together on the basis of charged interactions[11]. *In vivo*, MCs in the process of granulating build these structures incrementally, starting with the initial production of small granule subunits and followed by the fusion of these smaller subunits to build mature granules, each within a single vesicular membrane[11]. On degranulation, the vesicle fuses with the plasma membrane and the particle that it holds is released into the extracellular space to act as a slow-release depot of inflammatory mediators. In the context of biotechnology, complexes formed similarly (on the basis of charged interactions) and on a larger scale have been used for delivery of cytokines and nucleic acids *in vivo*[12–14]. To most closely approximate the particles that MCs release during degranulation (Fig. 1a) and replicate their efficient LN targeting[6], we have engineered our particles to consist of heparin, but complexed with chitosan, a non-immunogenic carbohydrate derived from crustacean shells that has significant technical advantages over other positively charged compounds. These components are both biocompatible and biodegradable[15,16]. We proposed that targeted delivery of cytokines in heparin–chitosan complexes would recapitulate the adjuvant activity of natural MC activation during infection *in vivo*.

Particles modelled after MC granules were formed by gradually adding a solution of heparin to a solution of chitosan in the presence of the cytokine TNF at acidic pH (Fig. 1b). As chitosan becomes protonated at acidic pH (ref. 17), modulation of the pH can influence the extent of complexation, control the size of aggregates and ensure the stability of particles when the solution is returned to neutral pH. Optimizing this parameter resulted in particles of relatively uniform size closely approximating the size of MC-derived particles (Fig. 1c,d and ref. 18). Particles were largely between 200 and 1,000 nm in diameter (Fig. 2a), and had a slightly positive zeta potential (Fig. 2b). They were stable without crosslinking within the range of physiologic pH, and only began to become disrupted, as determined by optical density, in extreme acidic or basic conditions (Fig. 2c). A small peak occurs in this curve around pH 4.5, which is the optimal pH for particle formation. The particles, therefore, seem to be the correct size to resemble MC-derived particles and be stable under circumstances approximating physiological conditions.

A major goal for these engineered particles was that they be able to incorporate cytokines within their structure, similar to MC granules. We expected that, on the basis of charged interactions, proteins, including our model cytokine, TNF, would bind to heparin in solution, facilitating entrapment within the forming heparin–chitosan matrix. To validate that TNF is efficiently packaged within the carbohydrate–particle backbone structure, we used a bioassay to measure TNF functional concentration, relying on TNF-induced cytotoxicity of the L929 cell line (Fig. 2d). As the

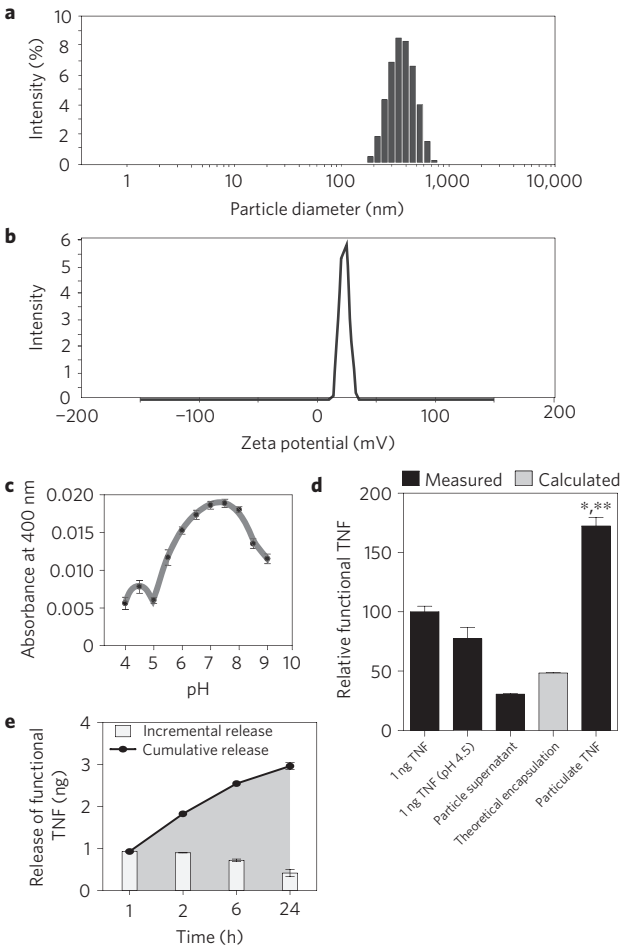

Figure 2 | Physical characteristics of synthetic particles, and mediator encapsulation. a,**b**, The size distribution (**a**) and zeta potential (**b**) of synthetic particles. **c**, The stability of particles under varying pH conditions determined by measuring the optical density of the solution. Note the peak that occurs around pH 4.5, where particles re-aggregate and form. Measurements in **a**–**c** were acquired using particles isolated and resuspended in water, and were made at room temperature. **d**, TNF-encapsulation efficiency was determined using a TNF cytotoxicity assay, based on TNF-induced killing of L929 cells. All values were compared with the functional activity of 1 ng of TNF, the amount added to the reaction mixture for encapsulation. Functional assessment of TNF enabled the activity of TNF lost during the protocol step of reaching pH 4.5 and returning to neutral pH to be determined. This and the remaining TNF in the reaction supernatant after particle formation and pelleting were used to calculate the TNF incorporated into the synthetic particles. The functional activity of the particulate fraction was greatly extended over 1 ng of soluble TNF ($*p = 0.0147$) and over theoretical soluble equivalent ($**p = 0.005$). **e**, The slow-release kinetics of TNF-loaded synthetic particles was determined over a 24 h period. At each designated time, particles were pelleted and the supernatant was removed and used to quantify the released TNF for that time interval using an L929 cytotoxicity assay. Graph bars represent the amount of TNF calculated to be released during the given time increment. These values were added to obtain the cumulative activity released during the experimental time course. Error bars represent s.e.m. in **c**–**e**.

particle formation reaction takes place under acidic conditions, we also investigated whether the pH shift of the solution to 4.5 for the duration of the experiment and back to neutral pH had any impact on TNF potency. Under these conditions, TNF retained ~80% of its functional activity (Fig. 2d). After precipitation of particles, the remaining soluble TNF in the supernatant was measured, and determined to be only 30% of the initial TNF in the reaction (Fig. 2d). Using this value and the measured loss of activity due to the pH change of the reaction, we calculated that particles formed under these conditions entrap approximately 50% of the functional TNF available in the reaction mixture (Fig. 2d). Measuring the activity of the particles demonstrated that particulate TNF is much more effective in promoting cytotoxicity than soluble TNF. On the basis of the 50% efficiency in particle loading, this study revealed that TNF encapsulation in heparin–chitosan particles extended its functional capabilities ~3.6-fold (Fig. 2d).

We presumed that the enhanced activity of particulate TNF over soluble TNF was due to its protection from degradation within the heparin–chitosan complex and its slow release during the 24 h assay. To determine if heparin–chitosan particles slowly release their cargo, we incubated TNF-loaded particles in tissue-culture conditions approximating physiological pH, salinity and temperature, and in the presence of serum proteins. At various times, the particles were pelleted from surrounding medium, which was saved to measure the released soluble TNF, and then resuspended in fresh medium. The incremental release of TNF over time was then measured by determining the functional TNF in the particle supernatant at each time (Fig. 2e). The appearance of functional TNF in the media supports the idea that these particles slowly release their cargo into soluble form over an extended time course (Fig. 2e).

In vivo LN targeting and particle-induced remodelling

To determine if our particles could replicate the functions and *in vivo* LN-targeting characteristics of natural MC-derived particles, we injected these particles into the rear footpads of mice, followed by isolating and examining the draining popliteal LN for their presence. To visualize the particles, during their synthesis we added a small amount of poly-L-lysine conjugated to the fluorochrome fluorescein isothiocyanate (PLL-FITC). The resulting particles were fluorescent and could be viewed in tissues by confocal microscopy after sectioning (Fig. 3a) and by epifluorescence in whole mount (Supplementary Fig. S1). In contrast, soluble PLL-FITC also drained to the LN; however, the staining was much more diffuse and dim than that of the labelled particles (Fig. 3a). Footpad-injected PLL-FITC particles quickly travel to the LN, where they can be seen in the subcapsular and medullary sinuses within minutes and with visually striking quantities apparent within 45 min (Fig. 3a). These appeared in a distribution pattern similar to that of peripherally released MC-derived particles, which were previously visualized within the LN sinuses[6]. We anticipate that these particles would also slowly release their cytokine cargo *in vivo* under physiological conditions because our experiments to investigate the kinetics of TNF sustained release were carried out under conditions designed to approximate the biochemical characteristics of the environment *in vivo* (Fig. 2d).

Furthermore, although some particles could be found inside cells, including DCs ($CD11c^+$), most of the particles did not co-localize with cellular markers CD11c or CD11b (Fig. 3b). Macrophages have been previously reported to line the subcapsular sinuses in the draining LNs (ref. 19) and to acquire soluble antigen from their location there[20,21], yet images of LNs containing synthetic particles suggest that DCs are much more efficient in taking up particles than macrophages ($CD11b^+CD11c^+$) within the LN (Fig. 3b). This assumption was also supported by flow cytometry data demonstrating that most of the earliest cells to acquire FITC-labelled particles were DCs. LN-resident DCs also acquired soluble FITC, but more macrophages or monocytes ($CD11b^+CD11c^-$) acquired this label than when FITC was injected in particulate form (Fig. 3c). As the image in Fig. 3b was acquired 30 min after peripheral injection, there should not be sufficient time for DC homing to LNs, which occurs significantly to the popliteal LN from the footpad only about 3 h after a peripheral insult[4]. Therefore, it seems that those

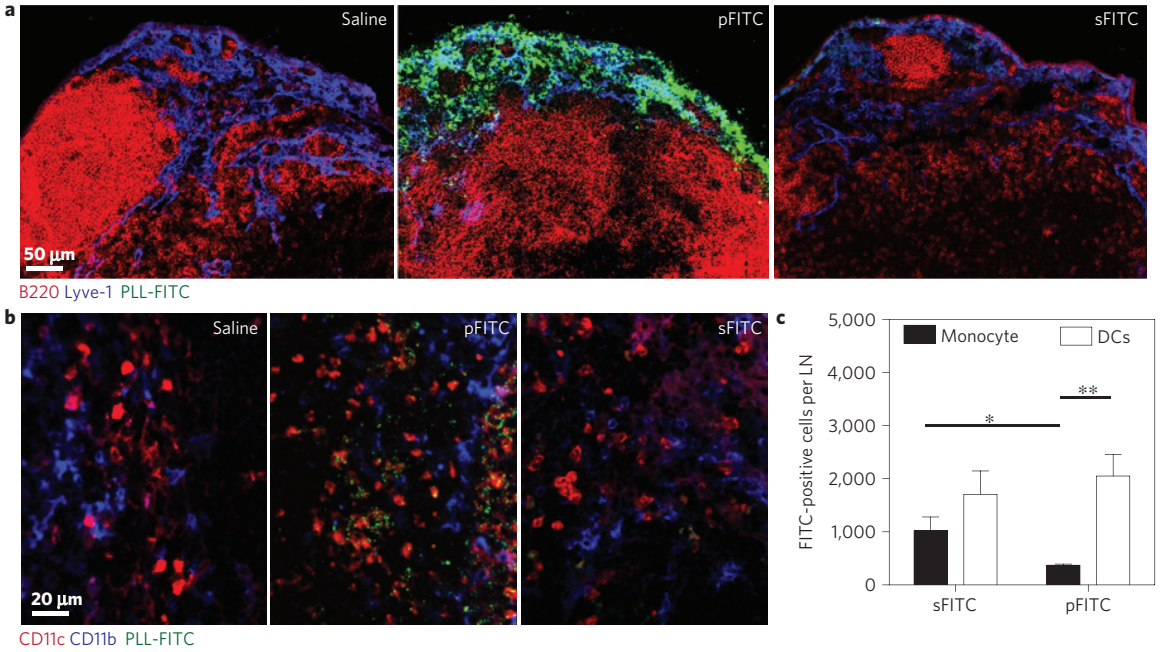

Figure 3 | Synthetic particles flow freely to the draining LN. a, LN sections after injection of particles containing PLL-FITC (pFITC), saline or soluble PLL-FITC (sFITC) are presented. These LNs were isolated 45 min post injection, sectioned, and stained for B cells (B220, red) and LN sinuses (Lyve-1, blue). The particles seem predominantly to be localized within the sinuses. **b**, LNs isolated 30 min after injection of saline, pFITC or sFITC were stained for CD11c (red) and CD11b (blue) to identify populations of phagocytic cells. Most particles are extracellular, although some co-localize with cells. For **a**,**b**, images were acquired by confocal microscopy. **c**, Quantitation of FITC-positive cells (monocytes, $CD11b^{+}CD11c^{-}$; DCs, $CD11c^{+}CD11b^{\pm}$) in draining LNs, 1 h after injection of pFITC or sFITC. Corresponding representative flow cytometry plots are contained in Supplementary Fig. S2b. Significantly fewer monocytes were $FITC^{+}$ after injection of pFITC versus sFITC ($^{*}p = 0.044$, determined by *t*-test). No significant difference was observed in the number of $FITC^{+}$ DCs between sFITC- and pFITC-injected animals. For pFITC-injected animals, more DCs were also $FITC^{+}$ than monocytes ($^{**}p = 0.0059$, determined by *t*-test). Error bars represent the s.e.m.

particles inside phagocytic cells were taken up within the LN. By 24 h, the number of cells containing particulate FITC had increased, yet DCs remained the dominant cell type (Supplementary Fig. S2a). Flow cytometry also revealed that particles were not measurably contained within non-phagocytic cell types lacking both CD11c and CD11b (Supplementary Fig. S2b). Having established the potential of our synthetic particles to travel to the LN, we next focused on assessing the functional effects of particulate TNF there.

Particulate TNF in the form of MC granules promotes LN remodelling, including swelling in response to infection[6]. This remodelling involves dynamic re-compartmentalization of cells and the development of new sub-structures, including germinal centres. Germinal centres contain activated B cells, as well as some DCs and T cells, and are highly consequential to the development of adaptive immune responses and to the production of high-affinity antibodies of multiple subclasses[22]. Therefore, we examined LNs to determine if particulate TNF in combination with an antigen could induce germinal centres. Mouse footpads were injected with a vaccine formulation containing the soluble experimental antigen haemagglutinin (HA) from the influenza virus (Flu), alone or in conjunction with particles containing TNF. Responses were also compared with mice administered HA emulsified in the standard vaccine adjuvant, alum, as a positive control. As other groups have reported that chitosan is able to induce innate immune activation on a cellular level[23], and that different formulations of chitosan complexes have adjuvant activity[24,25], we included a further control where mice were given HA in combination with empty particles, consisting of only the heparin–chitosan core. We then stained single-cell suspensions from the draining LN for the cellular activation marker of germinal centres, GL7, for quantification by flow cytometry. In this study, alum, but not soluble TNF or empty particles, showed expected adjuvant activity when compared with antigen alone, indicated by increased numbers of $GL7^{+}$ B cells in draining LNs, 10 days after vaccine administration (Fig. 4a). Similarly, our experimental adjuvant, TNF-loaded nanoparticles, also increased the numbers of germinal centre B cells (Fig. 4a). To visually confirm this quantitation of germinal-centre B cells, we stained LN sections for B-cell follicles, and show evidence of structures with germinal centre morphology at 10 days (Fig. 4b). In B-cell zones, GL7 staining was present, and a characteristic halo of reduced IgD staining on B cells, as occurs on activated B cells[26], was observed (Fig. 4b). We also observed similar results using a bacterially derived antigen, protective antigen from *Bacillus anthracis* (data not shown). These findings suggest that particulate TNF is sufficient to promote the production of germinal centres when administered in conjunction with a dose of antigen that would not otherwise induce their formation.

Particulate cytokines as vaccine adjuvants

On the basis of the observations that synthetic TNF-loaded particles show many of the physical characteristics and *in vivo* trafficking of natural MC-derived particles, and can also promote LN remodelling, we next investigated if the adjuvant activity of MC granules could be similarly recapitulated. To begin, we examined antibody production in response to a soluble antigen, HA derived from Flu, injected with particulate TNF or soluble TNF. To compare antibody quality after vaccination with a known adjuvant, we included a positive control of HA emulsified in alum. Mice were vaccinated, followed by a boost at 14 days, and serum was collected at 21 days to assess the resulting antibodies. When we measured total HA-specific IgG, we observed that particulate TNF, but not soluble TNF, showed adjuvant activity, as demonstrated by significantly increased antibody titres over antigen-alone vaccination, which were comparable to those elicited by the positive control, alum (Fig. 5a). Empty particles also did

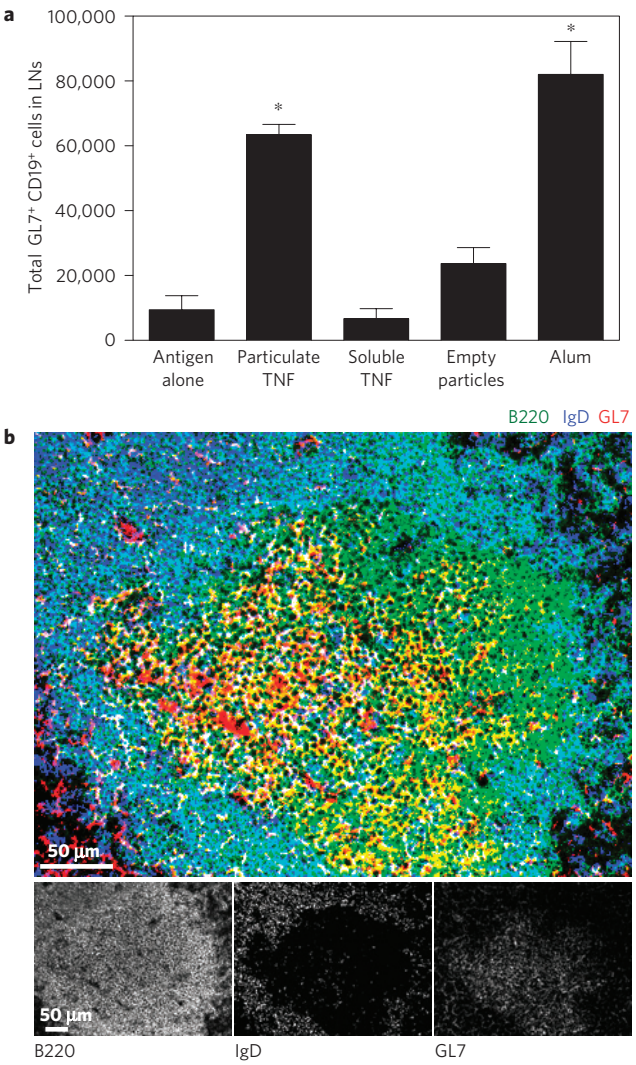

Figure 4 | Particulate TNF as an adjuvant promotes germinal-centre production. a, Numbers of activated B cells after immunization were quantified, where LNs were isolated 10 days after injection of mouse footpads with HA alone, or in combination with 1 ng of soluble TNF, or less than 1 ng of particulate TNF, or empty particles, or emulsified in alum. LN cells were stained for B cells (CD19) and the activation marker GL7 to quantify the number of germinal-centre B cells. Error bars represent the s.e.m., where $N = 3$–4 mice. Particulate TNF and alum significantly enhance numbers of germinal-centre B cells during vaccination; $p < 0.05$ by analysis of variance. The difference between particulate TNF and alum is not significant. **b**, A draining LN section, isolated 10 days after vaccination with 1 μg of HA in combination with less than 1 ng of encapsulated particulate TNF. Sections were stained for B cells (B220, green), IgD (blue) and GL7 (red) to reveal germinal-centre activity, including the characteristic halo of activated B cells that is revealed owing to their reduced surface expression of IgD. Individual channel series images are provided. Staining of positive and negative control groups is included as Supplementary Fig. S3.

not have adjuvant activity when combined with HA (Fig. 5a). This, combined with the observations in Fig. 4, support the idea that this low dose of highly purified and heparin-complexed chitosan is not sufficient to promote adjuvant activity. This contradicts the findings of others where adjuvant activity was observed using different formulations and/or higher doses of chitosan[24,25]. We found that, for both IgG1 and IgG2a subclasses, particulate TNF produced significantly increased antibody titres over antigen-alone vaccination (Fig. 5b), whereas alum promoted augmented IgG1 but not IgG2a endpoint titres after vaccination (Fig. 5c). This observation illustrates that particulate TNF may have further advantages over alum, promoting a broader specific antibody response. Individual antibody subclasses have been shown to have unique activities *in vivo* and differing effectivenesses against individual challenges[27]; therefore, the ability to promote antibody diversity is an important attribute of this adjuvant system.

As germinal centres, which we observe are promoted by particulate TNF (Fig. 4), are key for refining adaptive immunity and thought to be responsible for the generation of high-specificity antibody, we expected to also observe functional improvements in antibody quality after vaccination using particulate TNF as an adjuvant. To examine antibody avidity, we used a modified enzyme-linked immunosorbent assay (ELISA) procedure based on several published studies[28–31]. We found that the avidity of the antigen-specific antibodies that were present was much higher for mice given HA and particulate TNF when compared with mice given HA alone or with alum, whereas the avidities of the latter two controls were not dissimilar (Fig. 5d).

By using HA as our experimental antigen we were able to assess if our adjuvant system conferred any protection to the host in a lethal challenge model of Flu. For this study, mice were vaccinated as described previously, followed by challenge with a mouse virulent strain of Flu. When mice were monitored daily for survival, we observed that vaccination with HA in conjunction with particulate TNF significantly increased survival of mice after Flu challenge, to levels that did not differ from alum, which was used as a positive control (Fig. 5e). These data point to our particulate cytokine delivery system as an effective adjuvant that can be used to protect from an infectious challenge. Cumulatively, these studies demonstrate that this particulate TNF delivery system promotes both high-magnitude (Fig. 4a–c and high-affinity (Fig. 5d) antibodies as part of an adaptive immune response that can be protective, as in the case of a lethal Flu challenge (Fig. 5d), and that this response is possible by potentiating adaptive responses within the LN microenvironment (Fig. 4).

Differential particle loading to polarize immune responses

Although TNF was the target of our initial studies owing to its incorporation in natural MC-derived particles, other cytokines have been shown to have adjuvant activity[8] and could be potentially targeted to draining LNs by applying the MC's strategy. We sought to address the recognized shortfall of currently approved vaccine adjuvants in terms of their ability to capitalize on the remarkable plasticity of adaptive responses and to effectively direct immune outcomes differentially depending on the requirements of a unique challenge. Therefore, we encapsulated IL-12 in heparin–chitosan complexes, because this prominent DC-produced cytokine is important for driving cell-mediated immune responses that are essential to clear many viral infections[32]. Soluble IL-12 has also been previously employed to polarize immunity during immunization[33]. In our studies, injection of particulate IL-12 in conjunction with the soluble experimental antigen ovalbumin (OVA) greatly increased the number of LN T cells producing IFN-γ by 24 h, whereas an even larger amount of soluble IL-12 or particles alone did not (Fig. 6). This effect was further augmented in combination with particulate TNF (data not shown). These results demonstrate that differential loading of our synthetic particles may be an effective way to target minute quantities of cytokines to the draining LN during vaccination, and that the loaded cytokines need not conform to the template provided by MC granules. As a result, the cytokines delivered in particulate form and the resulting polarization of immune responses in the draining LN could be tailored to meet the requirements for protection against an individual challenge.

Much is required of an effective vaccine formulation, which would, ideally, consist of a single peptide, capable of conferring

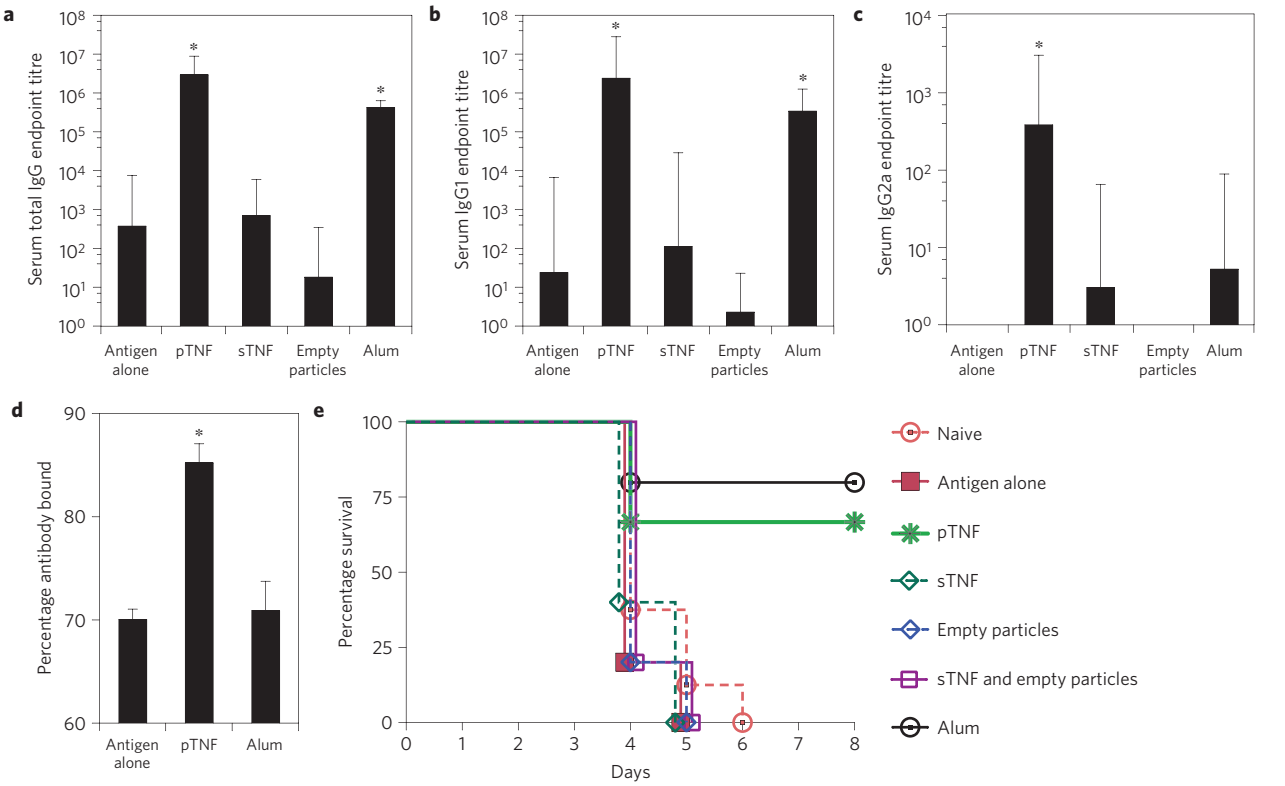

Figure 5 | Particulate TNF is an effective adjuvant that protects against a lethal flu challenge. a–c, Day 21 geometric mean titres for total IgG (**a**), IgG1 (**b**) and IgG2a (**c**) after vaccination with HA in combination with the designated adjuvants, with a boost at day 14. Data are pooled from two independent experiments; $n = 5$–10. TNF groups were vaccinated with 1 ng of soluble TNF, or less than 1 ng of particulate TNF per mouse. Significance was determined by one-way analysis of variance with Dunnet post-test to compare each group with the antigen-alone-group endpoint titres. Significance is represented by an asterisk, where $p < 0.05$. Error bars represent the s.d. (**d**) Day 21 serum (after vaccination with HA in combination with the designated adjuvants, with a boost at day 14), was tested to determine antibody avidity by washing ELISA plates with 0.25 M ammonium thiocyanate. The graph represents the percentage of antibody that remained bound to the plate after stringent washing, compared with normal ELISA washing. The avidity of antigen-specific antibodies was highest using particulate TNF as an adjuvant ($p < 0.05$), and did not differ between antigen alone and alum. Error bars represent the s.e.m.; $n = 5$ mice per group. **e**, Mice vaccinated as in **a**–**c** were challenged intranasally with a lethal dose of H1N1 Flu on day 35 (8×10^4 TCID-50 per mouse). Survival was monitored daily to generate the plot in **e**. For each group, $n = 5$–10 animals with data pooled from two independent experiments. Only synthetic particles containing TNF or the positive control, alum, increase survival significantly over naive mice or antigen-alone controls; for *p*-values for all comparisons, determined by log-rank test, see Supplementary Table S1.

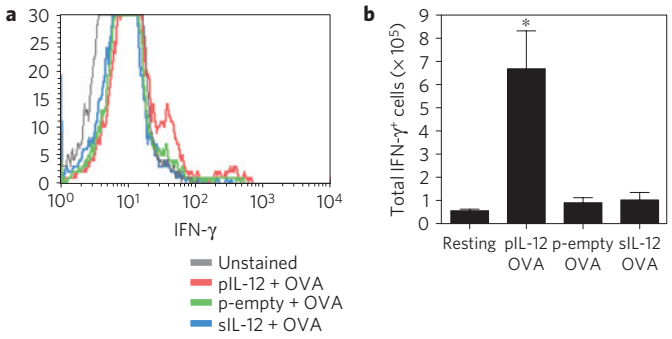

Figure 6 | Differential particle loading with IL-12 promotes Th1 polarized immunity. a, Delivery of particulate IL-12 (pIL-12) enhances IFN-γ production in draining LN T cells, 24 h after vaccination with OVA, in contrast to controls of soluble IL-12 (sIL-12) with OVA or empty particles (p-empty) with OVA. **b**, The total numbers of IFN-γ-producing cells. $p < 0.05$ and error bars signify the s.e.m., where $N = 3$.

protective immunity to the host. In reality, there is a large discrepancy between the events that occur in response to a single peptide and the events that break tolerance and promote active inflammation during and immunological memory after a true pathogenic challenge. For this reason, adjuvants are often incorporated into vaccines. Yet, even with adjuvants, vaccines frequently fall short of the ideal response required for protection, and for some challenges there exists no appropriate or effective adjuvant. Here, we have focused on extending the capabilities of cytokines because these natural non-immunogenic proteins are frequently the desired product of adjuvants[34], being able to directly promote adaptive immune responses. Even for common adjuvants, we are only just beginning to understand the underlying mechanisms of their efficacy[1,35], which are predominantly spatially confined to the peripheral site of vaccine administration and characterized by unique abilities to promote cytokine production or cellular activation[36]. Here, to investigate alternative means to enhance vaccine efficacy, we have looked to MCs, which can naturally catalyse and amplify adaptive immune responses[3,4,7,37], in part through their ability to produce particles that enable targeting of LNs and timed release by their inflammatory mediators[6]. Our particles seem to replicate the structure, biochemical attributes and functional capabilities of MC granules.

Particulate delivery of antigens as a strategy to promote their persistence or target LNs is a promising area of research within the efforts to improve vaccines. These endeavours have centred around the delivery of antigen to LNs or around targeting antigen for uptake by DCs and, largely, have used lipid or polymer-

based carriers[38]. Other groups have also employed particles for *in vivo* delivery of adjuvants[39–41]. It is our contention, however, that delivery of cytokines to LNs as a mechanism of modulating the microenvironment where the immune response is amplified and refined may enable the natural processing of peripherally administered antigen to proceed under conditions to optimize and maximize the adaptive immune response. However, as with MC-derived particles, some synthetic particles are able to persist within the tissue (data not shown), and these may also promote the function of encapsulated cytokines at the site of injection. Furthermore, although chitosan has been suggested to promote some level of innate immune activation[23], we find here that particles made from this highly purified chitosan do not, alone, have adjuvant activity, and this property emerges only when the particles are used as carriers for immuno-modulatory cytokines.

Furthermore, this technology confers a unique plasticity to the process of rational vaccine design owing to the potential of targeting precise combinations of cytokines to draining LNs to deliver the optimal combination for a unique challenge. MCs, too, have limited ability to modulate the content of their granules after a unique challenge, yet MC granules remain largely of the same composition[5]. By capitalizing on the encapsulation technology MCs have for promoting the persistence of cytokines and targeting them to the LN, we are able to differentially load these particles to enhance and also polarize the developing adaptive immune response. Particulate delivery of TNF to the LN during vaccination has also given some insight to the role this cytokine plays in the LN during the development of immunity, because we not only saw that antibody titres were increased after vaccination, but also observed that the avidity of these antibodies was greatly enhanced over antigen alone, and even over the standard adjuvant alum. This data suggests that particulate TNF can play a highly consequential role in ensuring antibody specificity during the initiation or refinement of adaptive immunity.

Methods

Particle synthesis and cytokine encapsulation. Chitosan (Vanson) was purified to drug grade by dissolving chitosan in 1% acetic acid overnight and filtering through Whatman paper in a Buchner funnel. The filtered solution was precipitated with NaOH and ultracentrifuged at 6,000 r.p.m. for 20 min. The chitosan pellet was washed with water and frozen at −80 °C before lyophilization. The purified chitosan used in these studies was 390 kDa with 83.5% deactylation. Synthetic heparin–chitosan particles were generated by gradually combining 1% heparin (Calbiochem) and 1% chitosan (both in dH_2O) in a 1:1 ratio at approximately pH 4.5. To produce particles, one volume of 1% chitosan was added to five volumes of 1% heparin and vortexed for 30 s. This was repeated until a 1:1 ratio of 1% chitosan to 1% heparin was achieved. After 10 min at room temperature, the pH was then adjusted to neutrality to prevent further aggregation. Particles were centrifuged at 14,000 × *g* for 10 min at 4 °C to form a pellet and washed with water before resuspension in PBS for injections or water for visualization on coverslips. To load particles with TNF, recombinant TNF (R&D Systems) was vortexed for 10 min in 1% heparin before the addition of chitosan. Differential loading of particles was achieved similarly by substituting recombinant IL-12 (R&D Systems). To label the particles for fluorescent tracking, 1 μg ml^{-1} of PLL-FITC was added to the 1% heparin before particle synthesis. For encapsulation studies, the amounts of TNF were measured using a standard L929 cytotoxicity assay. To determine the particle size distribution and zeta potential, particles were suspended in distilled, deionized water and measurements were taken using a Zetasizer Nano instrument (Malvern), according to the manufacturer's instructions.

Animal sources. Six-week-old female C57BL/6 mice were purchased from the National Cancer Institute. Sprague-Dawley rats were purchased from Taconic. All animals were housed at the Duke University Vivarium and all experimental protocols were approved by the Duke University Institutional Animal Care and Use Committee.

Particle-tracking studies and LN imaging. Synthetic particles containing FITC-PLL were injected in a maximum volume of 20 μl, and draining LNs were subsequently collected at the indicated times. Isolated popliteal LNs were flash-frozen in OCT (TissueTek), then cryostat-sectioned (10 μm) and fixed on slides with acetone for 15 min at 4 °C. Before initiating staining protocols, fixed, dried sections were rehydrated in PBS containing 1% BSA. The following primary antibodies were incubated overnight with tissue sections, as indicated in the figure legends: anti-B220-biotin, Rat-IgM anti-PNAd, anti-IgD-AlexaFluor647, anti-GL7-FITC, anti-CD11b and anti-CD11c (BD Biosciences). Slides were washed with PBS before secondary staining with antibodies or probes including streptavadin-Alexa546 (Molecular Probes), anti-rat-Cy3, anti-rat-IgM-FITC (Jackson Immunoresearch) and biotinylated anti-hamster (Pharmingen), followed by streptavadin-APC (BD Biosciences). Slides were mounted using ProLong Gold Antifade Reagent (Invitrogen). Images were prepared for publication using ImageJ software.

Vaccination studies and adjuvant activity evaluation. Mice were vaccinated with 1 μg of HA from influenza strain H1N1 A/New Caledonia/20/1999 (Protein Sciences). Antigen was prepared in a solution containing the appropriate adjuvant and injected in a 20 μl volume in a rear footpad. For particulate cytokine adjuvants, particles were produced as outlined above, followed by washing and resuspension in PBS for injection. For all particle injections a maximum of 10 μg of chitosan and 10 μg of heparin (assuming 100% efficiency of particle construction and no loss of material during washing) were injected per mouse. Assuming approximately 50% efficiency of encapsulation of cytokine (Fig. 1d), 0.5 ng of cytokine would have been injected into each mouse; however, this amount is represented as less than 1 ng because encapsulation efficiency can vary and because 1 ng per mouse was added to the reaction mixture during particle formation. Antigen and adjuvant were combined just before injection to limit antigen encapsulation in the particles. For alum, an emulsion was produced by mixing HA in 50% PBS, 50% alum (Sigma). Animals received a boost on day 14 and were bled on day 21. Serum was isolated and stored at −80 °C until ELISAs were carried out.

The survival curve was generated by challenging mice vaccinated as described above with a dose equivalent to 4×10^2 TCID50 of influenza A/PR/8/34 (serotype H1N1, Charles River). To infect, mice were briefly anesthetized with isolurane and Flu was instilled into the lungs through the nasal passages in a 40 μl volume of PBS. Before inoculation, this suspension of Flu and PBS was passed through a 0. 22 μm syringe filter. Mice were monitored daily for death or humane endpoints.

Statistics. For each vaccination study, significance was determined by one-way analysis of variance with Dunnet's post-test to compare treated groups with the control group. Significance for Kaplan–Meier curves was determined by the log-rank test. Further comparisons between two groups were carried out using Student's *t*-tests. Statistics were carried out using Excel and Prism software.

Received 15 July 2011; accepted 30 November 2011; published online 22 January 2012

References

1. Lambrecht, B. N., Kool, M., Willart, M. A. & Hammad, H. Mechanism of action of clinically approved adjuvants. *Curr. Opin Immunol.* **21,** 23–29 (2009).
2. Martín-Fontecha, A. *et al.* Regulation of dendritic cell migration to the draining lymph node: Impact on T lymphocyte traffic and priming. *J. Exp. Med.* **198,** 615–621 (2003).
3. McLachlan, J. B. *et al.* Mast cell-derived tumor necrosis factor induces hypertrophy of draining lymph nodes during infection. *Nature Immunol.* **4,** 1199–1205 (2003).
4. Shelburne, C. P. *et al.* Mast cells augment adaptive immunity by orchestrating dendritic cell trafficking through infected tissues. *Cell Host Microbe.* **6,** 331–342 (2009).
5. Abraham, S. N. & St. John, A. L. Mast cell-orchestrated immunity to pathogens. *Nature Rev. Immunol.* **10,** 440–452 (2010).
6. Kunder, C. A. *et al.* Mast cell-derived particles deliver peripheral signals to remote lymph nodes. *J. Exp. Med.* **206,** 2455–2467 (2009).
7. McLachlan, J. B. *et al.* Mast cell activators: A new class of highly effective vaccine adjuvants. *Nature Med.* **14,** 536–541 (2008).
8. Bradney, C. P., Sempowski, G. D., Liao, H. X., Haynes, B. F. & Staats, H. F. Cytokines as adjuvants for the induction of anti-human immunodeficiency virus peptide immunoglobulin G (IgG) and IgA antibodies in serum and mucosal secretions after nasal immunization. *J. Virol.* **76,** 517–524 (2002).
9. Perrillo, R. Benefits and risks of interferon therapy for hepatitis B. *Hepatology* **49,** S103–S111 (2009).
10. Anderlini, P., Przepiorka, D., Champlin, R. & Korbling, M. Biologic and clinical effects of granulocyte colony-stimulating factor in normal individuals. *Blood* **88,** 2819–2825 (1996).
11. Stevens, R. L. & Adachi, R. Protease–proteoglycan complexes of mouse and human mast cells and importance of their β-tryptase–heparin complexes in inflammation and innate immunity. *Immunol. Rev.* **217,** 155–167 (2007).
12. Roy, K., Mao, H. Q., Huang, S. K. & Leong, K. W. Oral gene delivery with chitosan–DNA nanoparticles generates immunologic protection in a murine model of peanut allergy. *Nature Med.* **5,** 387–391 (1999).
13. Kuang, M. *et al.* Phase II randomized trial of autologous formalin-fixed tumor vaccine for postsurgical recurrence of hepatocellular carcinoma. *Clin. Cancer Res.* **10,** 1574–1579 (2004).

14. Hanes, J. *et al.* Controlled local delivery of interleukin-2 by biodegradable polymers protects animals from experimental brain tumors and liver tumors. *Pharm. Res.* **18,** 899–906 (2001).
15. VandeVord, P. J. *et al.* Evaluation of the biocompatibility of a chitosan scaffold in mice. *J. Biomed. Mater. Res.* **59,** 585–590 (2002).
16. Lane, D. A. & Adams, L. Non-anticoagulant uses of heparin. *New Engl. J. Med.* **329,** 129–130 (1993).
17. Phaechamud, T., Koizumi, T. & Ritthidej, G. C. Chitosan citrate as film former: Compatibility with water-soluble anionic dyes and drug dissolution from coated tablet. *Int. J. Pharm.* **198,** 97–111 (2000).
18. Hammel, I., Lagunoff, D. & Galli, S. J. Regulation of secretory granule size by the precise generation and fusion of unit granules. *J. Cell Mol. Med.* **14,** 1904–1916 (2010).
19. Ingulli, E., Ulman, D. R., Lucido, M. M. & Jenkins, M. K. *In situ* analysis reveals physical interactions between $CD11b^{+}$ dendritic cells and antigen-specific CD4 T cells after subcutaneous injection of antigen. *J. Immunol.* **169,** 2247–2252 (2002).
20. Junt, T. *et al.* Subcapsular sinus macrophages in lymph nodes clear lymph-borne viruses and present them to antiviral B cells. *Nature* **450,** 110–114 (2007).
21. Phan, T. G., Grigorova, I., Okada, T. & Cyster, J. G. Subcapsular encounter and complement-dependent transport of immune complexes by lymph node B cells. *Nature Immunol.* **8,** 992–1000 (2007).
22. Klein, U. & Dalla-Favera, R. Germinal centres: Role in B-cell physiology and malignancy. *Nature Rev. Immunol.* **8,** 22–33 (2008).
23. Villiers, C. *et al.* From secretome analysis to immunology: Chitosan induces major alterations in the activation of dendritic cells via a TLR4-dependent mechanism. *Mol. Cell Proteomics* **8,** 1252–1264 (2009).
24. Sui, Z., Chen, Q., Fang, F., Zheng, M. & Chen, Z. Cross-protection against influenza virus infection by intranasal administration of M1-based vaccine with chitosan as an adjuvant. *Vaccine* **28,** 7690–7698 (2010).
25. Ghendon, Y., Markushin, S., Akopova, I., Koptiaeva, I. & Krivtsov, G. Chitosan as an adjuvant for poliovaccine. *J. Med. Virol.* **83,** 847–852 (2011).
26. Bhan, A. K., Nadler, L. M., Stashenko, P., McCluskey, R. T. & Schlossman, S. F. Stages of B cell differentiation in human lymphoid tissue. *J. Exp. Med.* **154,** 737–749 (1981).
27. Nimmerjahn, F. & Ravetch, J. V. Divergent immunoglobulin g subclass activity through selective Fc receptor binding. *Science* **310,** 1510–1512 (2005).
28. Pullen, G. R., Fitzgerald, M. G. & Hosking, C. S. Antibody avidity determination by ELISA using thiocyanate elution. *J. Immunol. Methods* **86,** 83–87 (1986).
29. Harris, S. L., Tsao, H., Ashton, L., Goldblatt, D. & Fernsten, P. Avidity of the immunoglobulin G response to a *Neisseria meningitidis* group C polysaccharide conjugate vaccine as measured by inhibition and chaotropic enzyme-linked immunosorbent assays. *Clin. Vaccine Immunol.* **14,** 397–403 (2007).
30. Marcus, H. *et al.* Contribution of immunological memory to protective immunity conferred by a *Bacillus anthracis* protective antigen-based vaccine. *Infect. Immun.* **72,** 3471–3477 (2004).
31. McCloskey, N., Turner, M. W. & Goldblatt, T. D. Correlation between the avidity of mouse–human chimeric IgG subclass monoclonal antibodies measured by solid-phase elution ELISA and biospecific interaction analysis (BIA). *J. Immunol. Methods* **205,** 67–72 (1997).
32. Stetson, D. B. & Medzhitov, R. Type I interferons in host defense. *Immunity* **25,** 373–381 (2006).
33. Afonso, L. C. *et al.* The adjuvant effect of interleukin-12 in a vaccine against *Leishmania major*. *Science* **263,** 235–237 (1994).
34. Mosca, F. *et al.* Molecular and cellular signatures of human vaccine adjuvants. *Proc. Natl Acad. Sci. USA* **105,** 10501–10506 (2008).
35. Datta, S. K. *et al.* Mucosal adjuvant activity of cholera toxin requires Th17 cells and protects against inhalation anthrax. *Proc. Natl Acad. Sci. USA* **107,** 10638–10643 (2010).
36. De Gregorio, E., D'Oro, U. & Wack, A. Immunology of TLR-independent vaccine adjuvants. *Curr. Opin. Immunol.* **21,** 339–345 (2009).
37. Galli, S. J., Nakae, S. & Tsai, M. Mast cells in the development of adaptive immune responses. *Nature Immunol.* **6,** 135–142 (2005).
38. Liang, M. T., Davies, N. M., Blanchfield, J. T. & Toth, I. Particulate systems as adjuvants and carriers for peptide and protein antigens. *Curr. Drug Deliv.* **3,** 379–388 (2006).
39. Kasturi, S. P. *et al.* Programming the magnitude and persistence of antibody responses with innate immunity. *Nature* **470,** 543–547 (2011).
40. Jewell, C. M., Lopez, S. C. & Irvine, D. J. *In situ* engineering of the lymph node microenvironment via intranodal injection of adjuvant-releasing polymer particles. *Proc. Natl Acad. Sci. USA* **108,** 15745–15750 (2011).
41. Singh, M. *et al.* Cationic microparticles are an effective delivery system for immune stimulatory cpG DNA. *Pharm. Res.* **18,** 1476–1479 (2001).

Acknowledgements

We thank C. A. Kunder, B. Berwin and A. Alonso for their contributions to producing the image in Fig. 1a. L. Eibist is thanked for her assistance in acquiring the EM of synthetic particles. We also thank A. P. S. Rathore and W. X. G. Ang for their manuscript review and discussions. The authors' work is supported by the US National Institutes of Health grants R01 AI96305, R01 AI35678, R01 DK077159, R01 AI50021, R37 DK50814 and R21 AI056101.

Author contributions

Experiments were designed by A.L.S. and S.N.A., with H.F.S. contributing to the experimental design of vaccination studies and K.W.L. contributing to the experimental design of studies relating to particle synthesis and characterization. Experiments were carried out by A.L.S. and C.Y.C. Data was analysed by A.L.S. and C.Y.C. with advice from S.N.A. and H.F.S. The manuscript was written primarily by A.L.S. All authors contributed to discussions and manuscript review.

Additional information

The authors declare no competing financial interests. Supplementary information accompanies this paper on www.nature.com/naturematerials. Reprints and permissions information is available online at http://www.nature.com/reprints. Correspondence and requests for materials should be addressed to A.L.S.